Molecular Crystals and Liquid Crystals

Publication details, including instructions for authors and subscription information:
http://www.tandfonline.com/loi/gmcl20

EXAFS Study of the Liquid Crystalline Phase of the Cyclopalladated 4-4′-bis(hexyloxy)azoxybenzene Acetylacetonate Complex

Oriano Francescangeli [a] , Claudio Ferrero [b] , Daniela Pucci [c] & Mauro Ghedini [c]

[a] Dipartimento di Scienze dei Materiali e della Terra and Istituto Nazionale per la Fisica della Materia, Università di Ancona, Ancona, Italy

[b] European Synchrotron Radiation Facility, Grenoble Cedex, France

[c] Dipartimento di Chimica, Università della Calabria, Arcavacata, Italy

Version of record first published: 18 Oct 2010

To cite this article: Oriano Francescangeli, Claudio Ferrero, Daniela Pucci & Mauro Ghedini (2002): EXAFS Study of the Liquid Crystalline Phase of the Cyclopalladated 4-4′-bis(hexyloxy)azoxybenzene Acetylacetonate Complex, Molecular Crystals and Liquid Crystals, 378:1, 77-88

To link to this article: http://dx.doi.org/10.1080/713738583

Mol. Cryst. Liq. Cryst., Vol. 378, pp. 77-88

1058-725X/02 $12.00 + .00
DOI: 10.1080/10587250290090057

EXAFS Study of the Liquid Crystalline Phase of the Cyclopalladated 4-4′-bis(hexyloxy)azoxybenzene Acetylacetonate Complex

ORIANO FRANCESCANGELI

Dipartimento di Scienze dei Materiali e della Terra and Istituto Nazionale per la Fisica della Materia, Università di Ancona, Ancona, Italy

CLAUDIO FERRERO

European Synchrotron Radiation Facility, Grenoble Cedex, France

DANIELA PUCCI and MAURO GHEDINI

Dipartimento di Chimica, Università della Calabria, Arcavacata, Italy

An EXAFS study of the mononuclear nematogenic cyclopalladated 4,4′-bis(hexyloxy)azoxybenzene complex in its liquid-crystalline phase is reported, aimed at exploring the metal coordination environment and confirming either the nature of intermolecular correlations or the presence of polar multimers. The interatomic distances between the palladium center and the atoms of the first coordination shell have been determined with an accuracy better than 10^{-2} Å. The results of the data analysis also indicate that the intermolecular interactions, if any, are very weak and do not involve the palladium(II) coordination sphere. In addition, they suggest that the aggregation model previously proposed to account for the ferroelectric behavior of this compound has to be revised to consider the possibility of either van der Waals and/or polar intermolecular interactions or a peculiar packing mode imposed by the P-shaped molecular geometry.

Keywords: EXAFS, liquid crystal, mononuclear cyclopalladated complex

Received 1 March 2001; accepted 19 April 2001.

It is a pleasure to thank Dr. A. Filipponi for his invaluable collaboration in performing the experiments and in the data analysis. Financial support from Italian Ministero per l'Università e la Ricerca Scientifica e Tecnologica (MURST) and Regione Calabria (POP 1994-99) is gratefully acknowledged.

Address correspondence to Prof. Oriano Francescangeli, Dipartimento di Scienze dei Materiali e della Terra and Istituto Nazionale per la Fisica della Materia, Università di Ancona, Via Brecce Bianche, I-60131 Ancona, Italy. E-mail: france@popcsi.unian.it

INTRODUCTION

The design of new molecular structures is a topical approach to materials for electrooptical and optoelectronic applications [1]. In pursuit of this end, we are currently concerned with the preparation of metal-containing liquid crystalline compounds [2]. In this field we have reported the synthesis of a mononuclear nematogenic complex, [LPd(acac)], Azpac in Figure 1, obtained by *ortho*palladation of the mesomorphic ligand 4,4′-bis(hexyloxy)azoxybenzene, HL [3].

Azpac is featured by an asymmetric "P-shaped" molecular geometry and unusually low transition temperatures (the nematic temperature range is 90°C–105°C), which allow extensive and unprecedented studies. Investigations on optical [4], viscoelastic [5], dielectric [6,7], and flexoelectric [8,9] properties were indeed carried out and, to gain a deeper knowledge of the structural and orientational properties in the mesophase, ^{2}H NMR spectroscopy measurements were performed [10].

With reference to practical applications, the electrooptical response and its thermal behavior, when subjected to different depolarization currents, were studied [11]. The results obtained revealed an unexpected transitory ferroelectric state normal to the molecular director. In order to explain this very interesting phenomenon, the existence of polar multimers was assumed. Accordingly, a simple model was suggested wherein the molecules are brought about by intermolecular interactions through the palladium center and the nitrogen-bonded oxygen atom of the azoxy group.

The most suitable experimental method to detect intermolecular interactions, both in the solid state and in the mesophase, is the extended X-ray

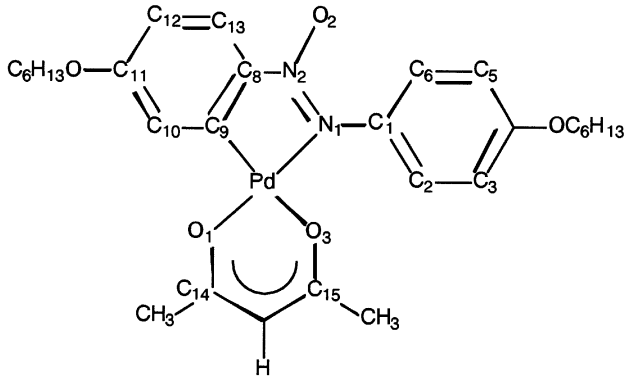

FIGURE 1 Molecular structure and atomic numbering scheme of Azpac.

absorption fine structure (EXAFS) technique. In this paper we report on the EXAFS study that we performed on the Azpac complex in order to explore the metal coordination environment and possibly confirm either the nature of intermolecular correlations or the presence of molecular multimers. Remarkably, this study represents one of the very few applications of the EXAFS analysis to metallomesogenic systems. In fact, it has been applied so far only to zinc and palladium alkoxydithiobenzoates complexes, where intradimer M-S interactions were investigated [12], to some dinuclear copper and rhodium carboxylates, for which a pseudopolymeric aggregation due to intermolecular M-O interactions was found both in the solid and in the discotic phases [13,14], and finally to copper salicylaldiminate complexes exhibiting intermolecular Cu-Cu correlations in the smectic B mesophase [15].

EXPERIMENT AND DATA ANALYSIS

Samples (about 50 mg) of Azpac were put into glass cells of lateral dimensions $10 \times 15\,\text{mm}^2$ and thickness 1 mm and carefully compressed with a small spatula until no cracks or holes were visible. The cells were inserted in a heating unit designed for X-ray absorption measurements [16]. The temperature was regulated within 1°C.

The EXAFS experiments were run on the XAFS beamline (BM29) [17] at the European Synchrotron Radiation Facility, Grenoble. The X-ray beam was obtained from the storage ring under the usual running conditions: 6.0 GeV, a maximum stored current of 200 mA, and a (311)-Si-double crystal monochromator. Data were collected in transmission mode. The sample was submitted to a monochromatic beam flux $\cong 10^9$ Ph/s. In order to assess possible radiation damage, spectra under the same temperature conditions were acquired as a function of time. They showed no modifications, thus implying no degradation of the samples. This was also confirmed by visual inspection of the samples. The direct and transmitted beam intensities were measured with ion chambers filled with argon, which is suitable for studies at the Pd K-edge. The spectral resolution $\Delta E/E$ during the experiments was estimated to be about 7.0×10^{-5} for a 0.2 mm slit aperture. The energy calibration was monitored using a palladium foil in conjunction with the samples of our palladium complex.

The EXAFS signal $\chi(k)$ corresponding to the atomic shell around the metal atom was extracted from the experimental absorption spectra $\mu(k)$

using the following normalization relation:

$$\chi(k) = (\mu - \mu_0)/\mu_0, \tag{1}$$

where μ_0 is the absorption coefficient of the isolated metal atom, $k = \sqrt{2m(E - E_e)}/\hbar$ is the modulus of the photoelectron wave vector, E is the photon energy, and E_e the energy edge (i.e., the threshold). The energy edge value was defined as being the energy corresponding to the maximum of the $\mu(E)$ derivative.

Data analysis was performed by using the GNXAS package [18,19], which takes into account the multiple scattering (MS) contributions. The GNXAS method is based upon a decomposition of $\chi(k)$ into a sum of different contributions:

$$\chi(k) = \sum_i \gamma^{(2)}(0,i) + \sum_{i,j} \gamma^{(3)}(0,i,j) + \cdots \sum_{i,j,\ldots,n} \gamma^{(n)}(0,i,j,\ldots,n) + \cdots. \tag{2}$$

Each contribution in this equation is associated to a n-atom configuration of the environment of the photoabsorber (0 indicates the photoabsorber and $i,j,\ldots,n$, the surrounding atoms). The $\gamma^{(n)}$ signals are the central quantities in the GNXAS approach and can be calculated by expanding them into appropriate MS series. In order to simulate the EXAFS signal of a given cluster of atoms using Eq. (2), a preliminary analysis of the main n-body configurations around the photoabsorber must be performed. An ab initio structural model is necessary to establish the most significant paths of the photoelectron.

The GNXAS approach for EXAFS data analysis is based on a fitting procedure that optimizes the matching between a model absorption signal $\mu_{\mathrm{mod}}(E)$ and the experimental signal $\mu(E)$. The model absorption signal, as a function of the photon energy E, is described in Filipponi and Di Cicco [19]. It should be mentioned here that $\mu_{\mathrm{mod}}(E)$ includes a smooth polynomial spline background accounting for the pre-edge region. The refinement of the structural parameters (bond lengths, bond angles, Debye-Waller-type factors) is done in the program using the following standard square residual function for the statistical analysis of the results [19]:

$$R_{sq}(\{\lambda\}) = \sum_{i=1}^{N} \frac{[\mu(E_i) - \mu_{\mathrm{mod}}(E_i;\lambda_1,\lambda_2,\ldots,\lambda_p)]^2}{\sigma_i^2}. \tag{3}$$

In Eq. (3) $\{\lambda\} = (\lambda_1,\ \lambda_2,\ldots,\lambda_p)$ is the set of p parameters on which μ_{mod} depends. It is assumed that the spatial distribution of the neighboring atoms

of Gaussian type. This procedure allows one to obtain reliable information on the atomic structure in the neighborhood of the photoabsorbed atom.

RESULTS AND DISCUSSION

EXAFS spectra of the Azpac complex at the Pd K-edge were recorded at different temperatures between 90°C and 105°C, the temperature range wherein the nematic phase occurs. As an example, Figure 2 shows the absorption spectrum measured at 98°C. No appreciable differences were observed among the spectra taken at different temperatures in the investigated range. The same could be stated for data collected at temperatures lower than 90°C, i.e., not in the nematic phase.

The data analysis required first the definition of an ab initio structural model in order to establish the most significant paths of the photoelectron. This was done by exploiting structural data concerning relevant bond distances, bond angles, and torsion angles around the photoabsorber in the isolated molecule that have resulted from the literature on model compounds, since a single crystal X-ray analysis of the Azpac molecule is not available. In particular, a set of reliable bond lengths and angles was obtained from the structural data of the related mononuclear cyclopalladated p-azoxyanisole 8-hydroxy-quinolinate and bis(acetylacetonate)palladium(II) complexes [20–21]. From these data, the distances between the Pd atom and the first neighboring atoms in the isolated Azpac (N1, C9, O1, O3) appear to be in the range 1.98–2.1 Å. On the other hand, based on the structural data

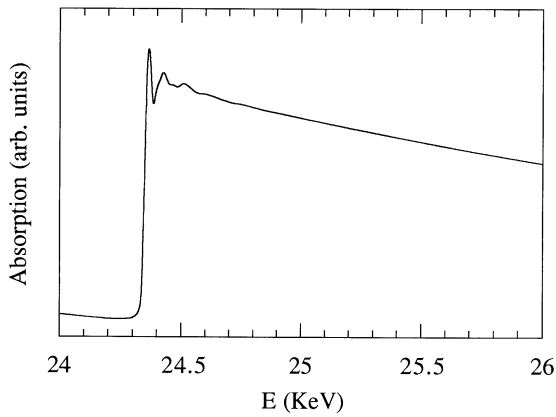

FIGURE 2 K-edge palladium EXAFS spectrum of Azpac at T = 98°C.

reported in Table 1 it is also possible to estimate the distances between the Pd core and the atoms of the same molecule which form the second coordination shell, with values ranging between 2.7 and 3 Å.

The possible presence of intermolecular interactions is expected to modify both the spatial extent and the coordination numbers of the first two coordination shells. In particular, a strong interaction that could bring the nitrogen-bonded oxygen of a molecule very close to the Pd core of the adjacent molecule at a distance comparable with those involved in the first coordination shell has to be considered. Indeed, based on the structural data of Table 1, as well as on steric considerations and on the literature data concerning non bonding M—O interactions [22], the minimum Pd—O(N) intermolecular distance should be comprised between 2.2 and 2.5 Å.

To prove the existence of such an interaction and also considering the complexity of the molecule that is mainly due to its high anisotropy, we have carried out the data elaboration as follows. First we restricted the analysis to a small cluster of atoms around the photoabsorber, including only the atoms of the first coordination shell of the isolated molecule. Accordingly, we set $n = 4$ for the coordination number, corresponding to the two oxygen atoms O1 and O3, the nitrogen N1, and the carbon C9 (Figure 1). The square residual function R_{sq} was then minimized with respect to the distances of the above four atoms from the Pd center. The results are reported in Table 2. The values of R and σ^2 represent the mean and variance for the bond length distributions of the atoms of the first coordination shell. The different components of the corresponding structural signal in k space are presented in Figure 3. The specific contributions to the overall $\chi(k)$ signal coming from the different atoms of the first shell are displayed from top to bottom and refer to the two-body Pd-O1 and Pd-O3 contributions $2 \times \gamma_1^{(2)}$, the Pd-C9 contribution $\gamma_2^{(2)}$, and the Pd-N1 contribution $\gamma_3^{(2)}$. The occurrence of the double term $2 \times \gamma_1^{(2)}$ in the upper curve of Figure 3 comes from the two indistinguishable oxygen atoms O1 and O3, thus resulting in the sum of two identical oxygen contributions. The two lower curves represent the comparison between the total model (sum of the four $\gamma^{(2)}$ contributions), and the experimental signal, and the calculated residual, respectively. The model signal is able to account for the low frequency part of the experimental EXAFS signal. The small residual values over essentially the whole k range being investigated strongly indicate that the EXAFS signal is mainly dominated by the contribution of the first coordination shell. This is confirmed by the result shown in Figure 4 where the Fourier transform of the experimental signal is compared with the theoretical Fourier transform calculated for the model cluster corresponding to Figure 3. In this figure

TABLE 1 Selected bond lengths (Å), bond angles (°), and torsion angles (°) assumed as ab initio structural model of Azpac; the atomic numbering scheme refers to the molecular structure of Figure 1

Bond distances (Å) from crystal structure determination [20]		*Bond angles (°) from crystal structure determination* [20]		*Torsion angles (°) from crystal structure determination* [20]	
Pd-N(1)	2.033(2)	N(1)-Pd-C(9)	80.1(1)	Pd-N(1)-N(2)-O(2)	178.0(2)
Pd-C(9)	1.984(3)	Pd-N(1)-N(2)	115.3(2)	Pd-N(1)-N(2)-C(8)	−3.0(3)
N(1)-N(2)	1.300(3)	N(1)-N(2)-C(8)	115.5(2)	N(1)-N(2)-C(8)-C(9)	−0.6(3)
N(2)-O(2)	1.258(3)	N(1)-N(2)-O(2)	123.4(2)	O(2)-N(2)-C(8)-C(9)	178.4(3)
N(2)-C(8)	1.429(3)	O(2)-N(2)-C(8)	121.1(2)	N(2)-C(8)-C(9)-Pd	3.9(3)
C(8)-C(9)	1.385(4)	N(2)-C(8)-C(9)	115.5(2)	C(8)-C(9)-Pd-N(1)	−4.1(2)
		Pd-C(9)-C(8)	113.5(2)	C(9)-Pd-N(1)-N(2)	4.0(2)
Bond distances (Å) from crystal structure determination [21]		*Bond angles (°) from crystal structure determination* [21]			
Pd-O(1)	1.985	O(1)-Pd-O(3)	94.91(6)		
Pd-O(3)	1.974	Pd-O(1)-C(14)	122.6(2)		

Estimated bond distances (Å) from crystal structure determination [20]

Pd-N(2)	2.84	Pd-C(8)	2.84	Pd-C(10)	3.08	Pd-C(14)	2.94	Pd-C(15)	2.97

*Standard deviations not reported.

TABLE 2 Results of the structural analysis of the Azpac EXAFS spectrum

	$R(\AA)$	$\sigma^2(\AA)^2$
Pd-0	1.99(1)	$4 \pm 1 \times 10^{-3}$
Pd-C	1.95(1)	$4 \pm 1 \times 10^{-3}$
Pd-N	2.08(1)	$4 \pm 1 \times 10^{-3}$

R and σ^2 are mean and variance, respectively, for the bond length distributions of the atoms of the first coordination shell. The figures in parentheses represent the statistical errors from the least-square refinement and refer to the least significant digit. The value of the square residual function is $R_{sq} = 0.2251 \times 10^{-6}$.

the continuous line represents the Fourier transform of the experimental $\chi(k)$ signal, the broken line is the theoretical Fourier transform given by the sum of the transforms of the signals of Figure 3 associated to the single atomic contributions, and the dashed line gives the residual [18,19]. The

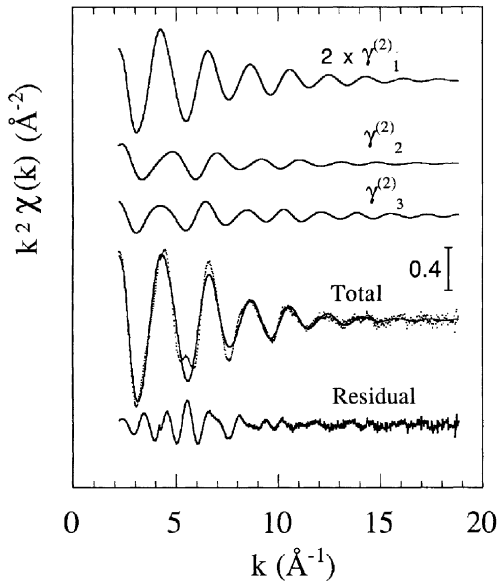

FIGURE 3 Prediction of the palladium K-edge EXAFS signal $\chi(k)$ of Azpac at T = 98°C, as obtained following the GNXAS approach for data analysis, considering a cluster including only atoms of the first coordination shell and assuming a coordination number $n = 4$. From top to bottom are reported: twice the two-body Pd-O contribution (Pd-O1 and Pd-O3) $\gamma_1^{(2)}$, the Pd-C9 contribution $\gamma_2^{(2)}$. the Pd-N1 contribution $\gamma_3^{(2)}$, the comparison between total model and experimental signal (dots), and finally the residual. The residual function contains essentially only statistical noise.

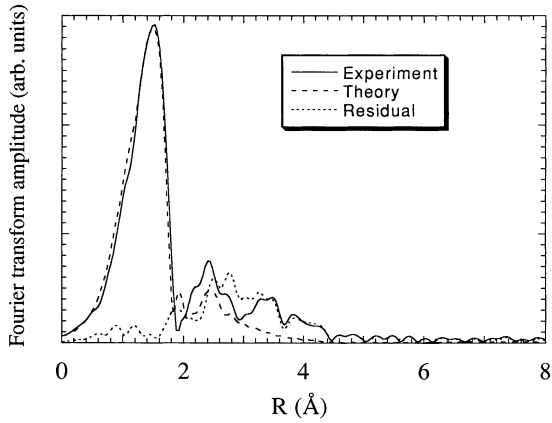

FIGURE 4 Fourier transform of the experimental EXAFS signal, compared with the theoretical Fourier transform as calculated from the model cluster corresponding to the spectrum of Figure 3. The continuous line is the Fourier transform of the experimental $\chi(k)$ signal, the broken line is the sum of the transforms of the signals of Figure 3 associated to the single atomic contributions, and the dashed line is the residual, i.e., the difference between experimental and theoretical curve.

satisfactory agreement between calculated and experimental spectrum, especially in the low-frequency region, indicated that the first shell model is essentially correct. However, it should be noted that the signals from the three shells have very similar frequencies, as all atoms considered are at approximately the same distance from the Pd atom. This entails a strong correlation between the fit parameters, suggesting that one must be extremely cautious while adding other parameters to the model, in as much as the error control in this case is likely to become problematic.

The second step of the data analysis was to repeat the data treatment described above, considering the presence of one additional oxygen atom, initially placed at about 2.1 Å in the shell of the first neighbors, and assuming $n = 5$ for the coordination number. This assumption accounts for the possibility of an intermolecular Pd—O(N) interaction that brings the nitrogen-bonded oxygen atom of a second molecule close to the first coordination shell in an axial position of the reference molecule. A cut-off distance of 3.0 Å for the interatomic distances to be refined was assumed in order to account for the possibility of an interaction weaker than the expected one, resulting in a bond length extending up to the second coordination shell. The corresponding best fit results for the EXAFS signal $\chi(k)$ are shown in Figure 5. The first three curves from the top refer to the intramolecular two-body Pd-O1/Pd-O3, Pd-C9, and Pd-N1 contributions,

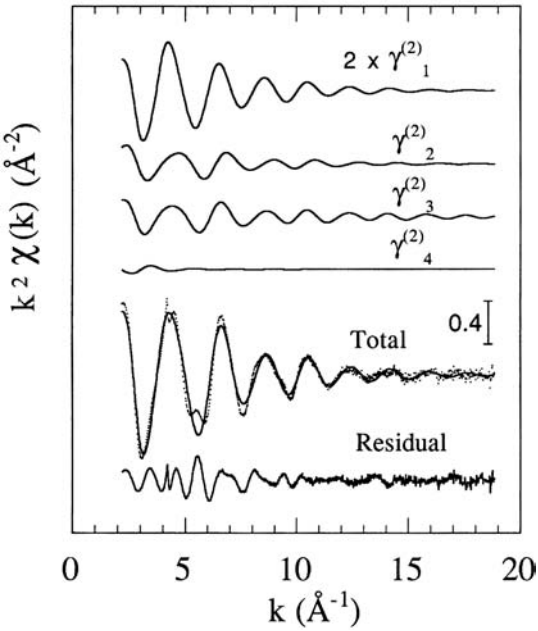

FIGURE 5 Prediction of the palladium K-edge EXAFS signal $\chi(k)$ of Azpac at T = 98°C, as obtained following the GNXAS approach for data analysis, assuming a first shell coordination number $n = 5$ to account for intermolecular interactions. From top to bottom are reported: twice the Pd-O contribution $\gamma_1^{(2)}$, the Pd-C9 contribution $\gamma_2^{(2)}$ the Pd-N1 contribution $\gamma_3^{(2)}$, the intermolecular two-body Pd-O(N) contribution $\gamma_4^{(2)}$, the comparison between total model and experimental signal (dots), and finally the residual (for comparison see the caption of Figure 4).

with the same notations as Figure 3. The additional curve $\gamma_4^{(2)}$ gives the intermolecular two-body Pd-O(N) contribution. As clearly shown by Figure 5, the latter term is absolutely negligible; in fact it is different from zero only in the low-frequency region $k < 5\,\text{Å}^{-1}$, where its amplitude, however, is to be confused with the statistical noise. In agreement with that, the best fit of the model signal provides intramolecular Pd-O1, Pd-O3, Pd-C9, and Pd-N1 distances that do not differ significantly (i.e., more than the statistical error) from those obtained with $n = 4$. In summary, the addition of a further oxygen atom to the shell of the nearest neighbors does not introduce any appreciable modification to the short-range structure.

It is important to observe that similar results were obtained irrespective of the nature of the additional extramolecular atom included in the shell of the nearest neighbors. In fact, even attempts made with palladium, nitrogen, and carbon introduced no significant modification to the short-range structure as obtained in the first data analysis step. This further consideration

suggests that not only Pd–O(N) but also no other detectable intermolecular interactions occur.

Finally, several attempts were made to determine the palladium interatomic distance of the second neighbors (multiple scattering analysis) since in the solid state single crystal X-ray investigations of dinuclear cyclopalladated azobenzene mesomorphic compounds have revealed that they are arranged in slippers pairs, with intermolecular nonbonding Pd—Pd contacts ranging from 3.668 to 3.758 Å [23,24]. However, these attempts did not give reliable results. In fact, due to the high asymmetry of the Azpac molecule, too many variables are involved in the minimization procedure. Under these conditions the probability of finding unrealistic values of the parameters minimizing the merit function is actually very high. It should also be reminded here that the relatively high experimental temperatures cause a significant broadening of the spatial distributions of the shell atoms, entailing a great uncertainty in the determination of their positions.

CONCLUSION

The interatomic distances between the palladium center and the four atoms which form the first coordination shell have been determined for the first time experimentally with an accuracy better than 10^{-2} Å. The four atoms are arranged in a square-planar geometry and exhibit distances from the metal center that compare well with the corresponding bond lengths usually detected at room temperature in similar cyclopalladated complexes. The accord between the findings of the present investigation and the theoretical prediction is also very good. In addition, the results of the data analysis suggest that the intermolecular interactions, if any, are presumably very weak and that they do not involve the palladium(II) coordination sphere. Accordingly, the aggregation model previously proposed [11] has to be revised. Either intermolecular interactions of Van der Waals and/or polar nature involving the whole Azpac molecules or a peculiar packing mode imposed by the ''P-shaped'' molecular geometry probably play a not negligible role in the formation of polar domains.

REFERENCES

[1] R. W. Gymer, *Endeavour*, **20**, 115–120 (1996).
[2] J. L. Serrano, ed., *Metallomesogens* (VCH, Weinheim, 1996).
[3] M. Ghedini, D. Pucci, S. Armentano, R. Bartolino, C. Versace, G. Cipparrone, and N. Scaramazza, Ital. Patent VE 92A000003, 16 Jan. 1992.

[4] (a) G. Cipparrone, C. Versace, D. Duca, D. Pucci, M. Ghedini, and C. Umeton, *Mol. Cryst. Liq. Cryst.*, **212**, 217–224 (1992).
(b) C. Versace, G. Cipparrone, D. Lucchetta, D. Pucci, and M. Ghedini, *Mol. Cryst. Liq. Cryst.*, **212**, 313–318 (1992).
[5] C. Versace, V. Formoso, D. Lucchetta, D. Pucci, C. Ferrero, M. Ghedini, and R. Bartolino, *J. Chem. Phys.*, **98(II)**, 8507–8513 (1993).
[6] N. Scaramuzza, M. C. Pagnotta, and D. Pucci, *Mol. Cryst. Liq. Cryst.*, **239**, 195–202 (1994).
[7] T. Beica, A. L. Alexe-Ionescu, A. Th. Ionescu, E. Miraldi, D. Pucci, and M. Rajteri, *Mol. Cryst. Liq. Cryst.*, **270**, 91–100 (1995).
[8] N. Scaramuzza and M. C. Pagnotta, *Mol. Cryst. Liq. Cryst.*, **239**, 263–267 (1994).
[9] A. G. Petrov, A. Th. Ionescu, C. Versace, and N. Scaramazza *Liq. Cryst.*, **19**, 169–178 (1995).
[10] L. Calucci, D. Catalano, M. Ghedini, N. L. Jones, D. Pucci, and C. A. Veracini, *Mol. Cryst. Liq. Cryst.*, **290**, 87–98 (1996).
[11] A. Th. Ionescu, D. Pucci, N. Scaramazza, C. Versace, A. G. Petrov, and R. Bartolino, *J. Chem. Phys.*, **103**, 5144–5148 (1995).
[12] D. Guillon, D. W. Bruce, P. Maldivi, M. Ibn-Elhaj, and R. Dhillon, *Chem. Mater.*, **6**, 182–189 (1994).
[13] M. Ibn-Elhaj, D. Guillon, A. Skoulios, P. Maldivi, A. M. Giroud-Godquin, and J. C. Marchon, *J. Phys. Paris*, **2**, 2237–2253 (1992).
[14] P. Maldivi, D. Guillon, A. M. Giroud-Godquin, J. C. Marchon, H. Abied, H. Dexpert, and A. Skoulios, *J. Chem. Phys.*, **86**, 1651–1664 (1989).
[15] G. Albertini, A. Guido, G. Mancini, S. Stizza, M. Ghedini, and R. Bartolino, *Europhys. Lett.*, **12**, 629–633 (1990).
[16] A. Filipponi and A. Di Cicco, *Nuclear Instrum. and Methods A*, **93**, 302–310 (1994).
[17] A. Filipponi, M. Borowski, D. T. Bowron, S. Ansell, A. Di Cicco, S. De Panfilis, and J. P. Itiè, *Rev. Sci. Inst.*, **71**(6), 2422–2428 (2000).
[18] A. Filipponi, A. Di Cicco, and C. R. Natoli, *Phys. Rev. B*, **52**, 15122–15134 (1995).
[19] A. Filipponi and A. Di Cicco, *Phys. Rev. B*, **52**, 15135–15149 (1995).
[20] M. Ghedini, S. Morrone, G. De Munno, and A. Crespini, *J. Organomet. Chem.*, **415**, 281–291 (1991).
[21] A. R. Siedle, T. J. Kistenmacher, R. M. Metzger, C. S. Kuo, R. P. Van Duyne, and T. Cape, *Inorg. Chem.*, **19**, 2048–2051 (1980).
[22] K. Nakajima, M. Kojima, S. Azuma, R. Kasahara, M. Tsuchimoto, Y. Kubozono, H. Maeda, A. Kashino, S. Ohba, Y. Yoshikawa, and J. Fujita, *Bull. Chem. Soc. Jpn.*, **69**, 3207–3216 (1996).
[23] A. Crispini, M. Ghedini, S. Morrone, D. Pucci, and O. Francescangeli, *Liq. Cryst.*, **20**, 67–76 (1996).
[24] M. Ghedini, D. Pucci, A. Crispini, I. Aiello, F. Barigelletti, A. Gessi, and O. Francescangeli, *Appl. Organomet. Chem.*, **13**, 565–581 (1999).